Effect of Dead Space on the Excess Noise Factor and Time Response of Avalanche Photodiodes

BAHAA E. A. SALEH, SENIOR MEMBER, IEEE, MAJEED M. HAYAT, STUDENT MEMBER, IEEE, AND MALVIN C. TEICH, FELLOW, IEEE

Abstract—The effect of dead space on the statistics of the gain process in continuous-multiplication avalanche photodiodes (APD's) is determined using the theory of age-dependent branching processes. The dead space is the minimum distance that a newly generated carrier must travel in order to acquire sufficient energy to cause an impact ionization. We derive analytical expressions for the mean gain, the excess noise factor, as well as the mean and standard deviation of the impulse response function, for the dead-space-modified avalanche photodiode (DAPD), under conditions of single carrier multiplication. The results differ considerably from the well-known formulas derived by McIntyre and Personick in the absence of dead space. Relatively simple asymptotic expressions for the mean gain and excess noise factor are obtained for devices with long multiplication regions. In terms of the signal-to-noise ratio (SNR) of an optical receiver in the presence of circuit noise, we establish that there is a salutatory effect of using a properly designed DAPD in place of a conventional APD. Finally, the relative merits of using a DAPD versus a multilayer (superlattice) avalanche photodiode (SAPD) are examined in the context of receiver SNR; the best choice turns out to depend on which device parameters are used for the comparison.

I. Introduction

Avalanche photodiodes (APD's) operate by converting a photo-generated carrier pair into a current pulse with sufficiently large charge to be detected by the electronic circuitry following the APD. The avalanche multiplication process introduces noise as a result of randomness in the positions at which secondary carriers are generated (position randomness), and as a result of randomness in the total number of carriers produced per initial photocarrier (gain randomness). This noise is in addition to the usual shot noise stemming from the Poisson photon nature of light, and the electronic noise of the circuitry; like these factors it too contributes to the degradation of optical receiver sensitivity. Expressions have long been available for the mean gain, excess noise factor, and impulse response function for continuous multiplication (conventional) APD's [1]–[7] and for multilayer (superlattice) APD's, which are usually denoted as SAPD's [8]–[11].

A fundamental assumption implicit in most models of the noise behavior of conventional APD's [1]–[7] is that the impact ionization probability of a carrier is the same at all times, including the instant following its birth, so that this probability is independent of the carrier's history. From a physical point of view, however, a newly generated carrier must travel some distance in order to build up energy sufficient to enable it to initiate an ionization. To accommodate this requirement, we formulate a multiplication model in which the ionization probability of a carrier is set to zero for a certain distance (called the dead space) immediately following its generation. More realistically, the ionization probability would be expected to decline following birth and then gradually increase over some distance (implying a sick space), rather than decreasing precisely to zero for a fixed space (implying a dead space). However, the simpler dead-space model adequately captures the essence of the effect while reducing the mathematical complexity to a minimum.

Using the dead-space model, Okuto and Crowell [12], [13] accounted for its effects by replacing the conventional ionization coefficient with a nonlocalized coefficient incorporating memory. They calculated the mean gain for a single-carrier injection (SCI) double-carrier multiplication (DCM) APD by obtaining numerical solutions to recursive equations. LaViolette [14] and LaViolette and Stapelbroek [15] studied the statistics of SCI single-carrier multiplication (SCM) APD's in the presence of sick space. They described the multiplication in terms of a non-Markovian binary age-dependent branching process. By using numerical techniques they determined the mean, excess noise factor, higher moments, and probability distribution of the number of carriers, all as functions of the multiplication region length.

In this paper, we examine the statistics of the multiplication process for an SCI/SCM APD incorporating dead space. We consider the multiplication process in terms of an age-dependent branching process and use Laplace transform methods to obtain analytical expressions for the mean gain and for the excess noise factor. Analytical expressions for the asymptotic values of the mean gain and excess noise factor are also derived in terms of the

Manuscript received November 20, 1989; revised April 29, 1990. This work was supported by the National Science Foundation. The review of this paper was arranged by Associate Editor G. Craford.

B. E. A. Saleh and M. M. Hayat are with the Department of Electrical and Computer Engineering, University of Wisconsin, Madison, WI 53706-1691.

M. C. Teich is with the Center for Telecommunications Research, Department of Electrical Engineering, Columbia University, New York, NY 10027.

IEEE Log Number 9036877.

Malthusian parameter of the branching process [16]–[18] in the limit when the length of the multiplication region is much greater than the dead space.

We demonstrate that the SNR of an optical receiver is enhanced by the use of a DAPD rather than an APD. On the other hand, the DAPD optical receiver may, or may not, outperform the SAPD receiver, depending on the selection of the SAPD device parameters used for the comparison. The operation of the two devices differs in a fundamental way: SAPD multiplication is locked to lattice positions determined by the material structure alone whereas DAPD multiplication is locked to locations determined by the carrier births alone.

Finally, we examine the properties of the DAPD impulse response as a function of the time following photoexcitation. We derive an expression for the mean current response which takes the form of an integral that is numerically evaluated. In the asymptotic case, when the length of the multiplication region is much larger than the dead space, analytical expressions for the mean and standard deviation of the response as functions of time are obtained.

The SCM assumption implicit in our calculations limits the usefulness of our results to devices with large electron-to-hole ionization ratios. Certain continuous materials such as Si, and multilayer devices of certain materials [8]–[11], [19]–[25], effectively operate in this mode. Though it may possibly be tractable, an analytic solution of the problem of noise in DCM APD's with dead space has not yet been set forth. An analysis similar to that carried out here can be extended to the sick-space model.

II. Model

The device under consideration is a single-carrier injection single-carrier continuous multiplication (SCI/SCM) avalanche photodiode. Let l be the length of the multiplication region and d the dead space. An electron is injected at the edge of the multiplication region ($x = 0$). It travels a distance d without ionizing, after which it may ionize with probability density (per unit length) α, the electron ionization coefficient. Upon ionization, an electron–hole pair is created. The electron and hole travel in opposite directions under the effect of the electric field, with fixed velocities v_e and v_h, respectively. The original and newly created electrons travel in the same direction and repeat the same process independently and identically, and so on. This process continues until all the electrons reach the end of the multiplication region ($x = l$).

Let $Z(x)$ denote the total number of electrons at position x at time x/v_e. By determining the statistical properties of the stochastic process $Z(x)$, we will be able to determine the statistics of the APD gain $G = Z(l)$ as well as the statistics of the stochastic impulse response function $i(t)$. Let $i_p(t, x)$ be the electric current pulse, in the external circuit, induced by an electron–hole pair created at position x; then [10]

$$i_p(t, x) = i_e(t, x) + i_h(t, x) \tag{1a}$$

where

$$i_e(t, x) = \frac{qv_e}{l}\left\{u\left(t - \frac{x}{v_e}\right) - u\left(t - \frac{l}{v_e}\right)\right\} \tag{1b}$$

and

$$i_h(t, x) = \frac{qv_h}{l}\left\{u\left(t - \frac{x}{v_e}\right) - u\left(t - \frac{x}{v'}\right)\right\} \tag{1c}$$

are the components due to the created electron and hole, respectively, $u(x)$ is the unit step function, q is the electron charge, and $1/v' = (1/v_e) + (1/v_h)$. The impulse response function $i(t)$ is then given by the stochastic integral

$$i(t) = \int_0^l i_p(t, x)\, d(Z(x)). \tag{1d}$$

III. Statistics of the Gain

The stochastic process $Z(x)$, that represents the number of electrons at position x, will be shown to be describable by an age-dependent branching process. For convenience, we begin with a brief review of these processes [16]–[18].

An age-dependent branching process $Y(t)$ represents an evolving population of particles. The process is initiated at time $t = 0$ with a parent particle. After a random time T (the age), this particle gives birth to k offsprings with probability P_k, $k = 0, 1, 2, \cdots$, and dies in the process. Each of the offsprings behaves exactly in the same manner. The ages of all particles are statistically independent and identically distributed random variables with probability density function $h(T)$. The ages are also independent of the number of offsprings created at any stage.

The process $Z(x)$ is a special case of the age-dependent branching process with x replacing t. The process starts at $x = 0$ with one electron, $Z(0) = 1$, which traverses a random distance X_a called the lifespan (analogous to the age T), after which it dies in the process, giving birth to two electrons with probability one. Thus $P_k = 1$ for $k = 2$, and zero, otherwise. The two electrons behave exactly the same way, and so on. The process terminates when all electrons reach the end of the multiplication region ($x = l$). The lifespan X_a has a probability density function $h(x_a)$. In the case of multiplication with a fixed dead space d

$$h(x_a) = \begin{cases} 0, & x_a \le d \\ \alpha e^{-\alpha(x_a - d)}, & x_a > d. \end{cases} \tag{2}$$

We now proceed to determine the statistical properties of $Z(x)$ drawing freely from the literature on age-dependent branching processes [16], [17].

A. Probability Distribution

Let $P_z(k, x)$, $k = 1, 2, 3, \cdots$, denote the probability that $Z(x) = k$. Since the multiplication region is assumed to be homogeneous, the probability that an electron at position x_1 produces k electrons at position $x_2 > x_1$ is $P_z(k, x_2 - x_1)$. If $Z(x) = k$, $k > 1$, and if the first ionization (death) occurs at position $\xi \le x$, then the two electrons generated at ξ must produce k electrons in total in the remaining distance $x - \xi$. Since each of the two electrons acts independently, the probability that the two produce a total of k is the discrete convolution

$$\sum_{i=1}^{k-1} P_z(k-i, x-\xi) P_z(i, x-\xi).$$

By averaging over all ξ we obtain an integral equation for $P_z(k, x)$, for $k > 1$, given by

$$P_z(k, x) = \int_0^x h(\xi) \sum_{i=1}^{k-1} P_z(k-i, x-\xi) \cdot P_z(i, x-\xi)\, d\xi, \qquad k > 1. \tag{3}$$

For $k = 1$

$$P_z(k, x) = 1 - H(x) \tag{4}$$

where

$$H(x) \equiv \int_0^x h(\eta)\, d\eta$$

is the distribution function for the lifespan.

Equation (3) for $P_z(k, x)$ is solved by use of the generating-function (gf) technique. The mgf is defined by

$$F_z(s, x) = \sum_{k=1}^{\infty} P_z(k, x) s^k, \qquad |s| \le 1 \tag{5}$$

and will be used to determine the moments of $Z(x)$. By inserting (3) and (4) into (5) we obtain an integral equation which recursively defines $F_z(s, x)$

$$F_z(s, x) = s(1 - H(x)) + \int_0^x h(\xi) F_z^2(s, x-\xi)\, d\xi. \tag{6}$$

We thus have a nonlinear integral equation involving no summations, which we must solve for $F_z(s, x)$. Although there is no explicit solution to this equation, it is readily used to generate the moments of the process $Z(x)$.

B. Mean Gain

The mean of $Z(x)$, $\mu(x) = E\{Z(x)\}$, is the derivative of the gf evaluated at $s = 1$

$$\mu(x) = \left.\frac{\partial F_z(s, x)}{\partial s}\right|_{s=1}.$$

Using (6), we obtain an integral equation for $\mu(x)$

$$\mu(x) = 1 - H(x) + 2\int_0^x \mu(x-\xi) h(\xi)\, d\xi. \tag{7}$$

The mean gain $\overline{G}$ is simply given by $\mu(l)$.

Since the above integral is a convolution, the use of the Laplace transforms

$$\hat{M}(\sigma) = L\{\mu(x)\} = \int_0^\infty \mu(x) e^{-\sigma x}\, dx$$

and

$$\hat{H}(\sigma) = L\{h(x)\}$$

allows us to express $\hat{M}(\sigma)$ as

$$\hat{M}(\sigma) = \frac{1 - \hat{H}(\sigma)}{\sigma[1 - 2\hat{H}(\sigma)]}. \tag{8}$$

In the fixed dead space case for which h is given by (2), $\hat{M}(\sigma)$ becomes

$$\hat{M}(\sigma) = \frac{1 + \sigma - e^{-D\sigma}}{\sigma(1 + \sigma - 2e^{-D\sigma})} \tag{9}$$

where we have used the scaled distance $X = \alpha x$ and the scaled dead space $D = \alpha d$. $\mu(X)$ can be computed by taking the inverse Laplace transform of $\hat{M}(\sigma)$, which can be carried out numerically. The expression for $\hat{M}(\sigma)$ in (9) matches the Laplace transform of the expression obtained by Okuto and Crowell [12] using a recursive method. Their method is applicable only to the mean, however.

C. Variance and Excess Noise Factor

The second moment $\mu_2(x) = E\{Z^2(x)\}$ can be determined from the relation

$$\mu_2(x) = \left.\frac{\partial^2 F_z(s, x)}{\partial s^2}\right|_{s=1} + \mu(x). \tag{10}$$

By using (6), it can be shown [16] that $\mu_2(x)$ satisfies the integral equation

$$\mu_2(x) = 1 - H(x) + 2\int_0^x [\mu^2(x-\xi) + \mu_2(x-\xi)] h(\xi)\, d\xi. \tag{11}$$

Using the Laplace transform $\hat{M}_2(\sigma) = L\{\mu_2(x)\}$, (11) gives

$$\hat{M}_2(\sigma) = \frac{1 - \hat{H}(\sigma)[1 - 2\sigma\hat{m}(\sigma)]}{\sigma[1 - \hat{H}(\sigma)]} \tag{12}$$

where

$$\hat{m}(\sigma) = L\{\mu^2(x)\}. \tag{13}$$

In the fixed dead space case, we obtain

$$\hat{M}_2(\sigma) = \frac{1 + \sigma + e^{-D\sigma}[\sigma\hat{m}(\sigma) - 1]}{\sigma(1 + \sigma - 2e^{-D\sigma})} \tag{14}$$

which can be Laplace inverted numerically to give $\mu_2(X)$.

The variance of the gain is then $\mathrm{Var}(G) = \mu_2(l) - \mu^2(l)$. The factor

$$F(x) = \frac{\mu_2(x)}{\mu^2(x)} \tag{15}$$

evaluated at $x = l$, is the excess noise factor of the APD.

The autocorrelation function

$$R(x_1, x_2) = E\{Z(x_1)Z(x_2)\}$$

may also be derived using a similar approach. We provide an expression for $R(x_1, x_2)$ only in the asymptotic case, to be discussed next.

D. Asymptotic Results

In accordance with the theory of age-dependent branching processes, the first and second moments, $\mu(x)$ and $\mu_2(x)$, become asymptotically exponential functions of x as $x \to \infty$ [16]

$$\mu(x) \sim C_1 e^{\beta x} \quad (x \gg d) \tag{16}$$

and

$$\mu_2(x) \sim C_2 e^{2\beta x} \quad (x \gg d) \tag{17}$$

where β is the Malthusian parameter of the age-dependent branching process. The parameter β is the solution to the Malthusian equation

$$2\int_0^\infty e^{-\beta y} h(y)\, dy = 1. \tag{18}$$

The constants C_1 and C_2 are given by

$$C_1 = \frac{1}{2\beta \int_0^\infty y e^{-\beta y} h(y)\, dy} \tag{19}$$

and

$$C_2 = \frac{2C_1^2 \int_0^\infty e^{-2\beta y} h(y)\, dy}{1 - 2\int_0^\infty e^{-2\beta y} h(y)\, dy}. \tag{20}$$

The asymptotic excess noise factor is independent of x, and is given by

$$F(x) \approx \frac{C_2}{C_1^2} \triangleq F_\infty. \tag{21}$$

The asymptotic autocorrelation function is

$$R(x_1, x_2) \sim C_2 e^{\beta(x_1 + x_2)} \quad (x_1 \gg d,\ x_2 \gg d) \tag{22}$$

so that the random variables $Z(x_1)$ and $Z(x_2)$ are asymptotically fully correlated.

In the fixed dead space case

$$C_1 = \frac{B + 1}{2B(DB + D + 1)} \tag{23}$$

$$C_2 = \frac{C_1^2 (B+1)^2}{1 + 2B - B^2} \tag{24}$$

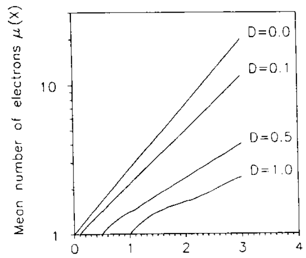

Fig. 1. Mean value of the number of electrons $\mu(X)$ as a function of the scaled distance $X = \alpha x$, for different values of the scaled dead space parameter $D = \alpha d$. These functions are asymptotically exponential.

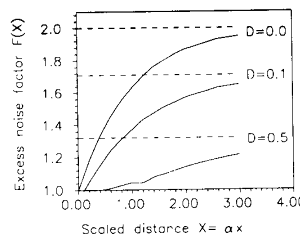

Fig. 2. Excess noise factor F as a function the scaled distance $X = \alpha x$ for different values of the scaled dead space parameter $D = \alpha d$. The dashed lines represent the corresponding asymptotic values F_∞.

where $B = \beta/\alpha$ is the scaled Malthusian parameter and it is the solution to the equation

$$2e^{-DB} - B = 1 \tag{25}$$

and where the reader is reminded that $D = \alpha d$ is the scaled dead space.

We will discuss the results for the fixed dead space case. The scaled Malthusian parameter B in (25) approaches 1 as D approaches 0. Figs. 1 and 2 depict the exact behavior of $\mu(X)$ and the exact and asymptotic behavior of $F(X)$, respectively, for different values of D. Convergence to asymptotic values is faster as D approaches 0. For large D, F is a nonmonotonic function in the vicinity of the origin. This effect increases with increase of D. When $D = 0$, the process is the usual Markovian (continuous) branching process for which $\mu(X)$ is exponential and $F(X)$ approaches 2 monotonically. It is also seen that both $\mu(X)$ and $F(X)$ decrease in magnitude for all X as D increases. In Fig. 3, the exact and asymptotic excess noise factor F are plotted as functions of the mean gain $\overline{G}$. Fig. 4 is a plot of the asymptotic excess noise factor F_∞ as a function of D. It shows that F_∞ drops from 2 to 1 as D varies from 0 to ∞.

E. Signal-to-Noise Ratio

Although the presence of dead space has the advantage of reducing the excess noise factor, this is accompanied by a reduction in the mean gain, so that it is not clear whether dead space improves the performance of an optical receiver. We proceed to show that it does indeed.

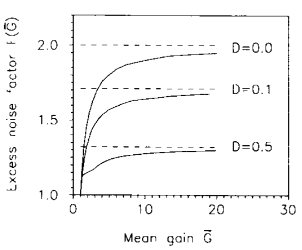

Fig. 3. Dependence of the excess noise factor F on the mean gain $\overline{G}$ for different values of the scaled dead space parameter $D = \alpha d$. The dashed lines represent the corresponding asymptotic values F_∞.

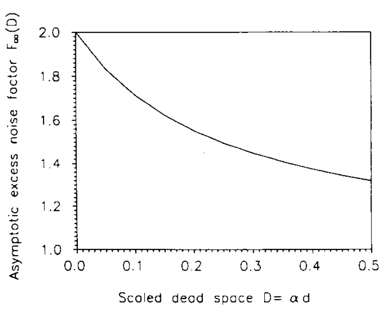

Fig. 4. Dependence of the asymptotic excess noise factor F_∞ on the scaled dead space parameter $D = \alpha d$.

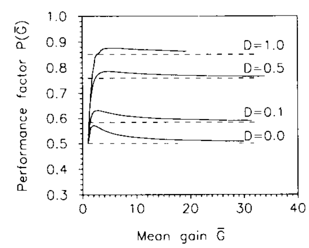

Fig. 5. The performance factor P as a function of the mean gain $\overline{G}$ for different values of the scaled dead space parameter $D = \alpha d$. The dashed lines represent the corresponding asymptotic ($\overline{G} \to \infty$) values P_∞. The circuit-noise parameter $\sigma^2/\phi T$ is assumed to be 1. The receiver signal-to-noise ratio is proportional to P.

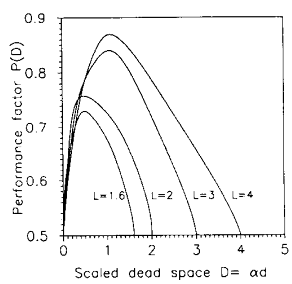

Fig. 6. The performance factor P as a function of the scaled dead space parameter $D = \alpha d$ for different values of the scaled multiplication region length $L = \alpha l$. The circuit-noise parameter $\sigma^2/\phi T$ is assumed to be 1.

The simplest measure of performance is the signal-to-noise ratio (SNR). Consider a digital communication system receiving a photon flux ϕ (photons per second). Assuming Poisson photon statistics, the SNR of the total charge accumulation in the detection circuit in a time interval T is given by [26]

$$\text{SNR} = \frac{\phi T \overline{G}^2}{\overline{G}^2 F + \dfrac{\sigma^2}{\phi T}} \tag{26}$$

where σ^2 is the variance of the circuit noice charge (in units of number of electrons) and the quantum efficiency of the APD is assumed to be unity. If an analog receiver is used instead, then (26) remains applicable provided that $T = 1/2B$ where B is the receiver bandwidth. The factor ϕT is the SNR for an ideal photon-noise limited receiver. The performance factor

$$P = \frac{\overline{G}^2}{\overline{G}^2 F + \dfrac{\sigma^2}{\phi T}} \tag{27}$$

therefore represents the SNR reduction due to gain fluctuations and circuit noise. The dependence of this factor on the dead space is implicit in F and $\overline{G}$, as discussed earlier.

Fig. 5 displays the performance factor P versus the mean gain $\overline{G}$ for fixed values of the circuit-noise parameter $\sigma^2/\phi T$ and for different values of D. For a given mean gain $\overline{G}$ and a specified value of $\sigma^2/\phi T$, the performance improves, since F decreases, with increasing D. For $D = 0$, P increases at first as a function of $\overline{G}$, and then decreases reaching an asymptotic value of $\frac{1}{2}$ since $F_\infty = 2$. For $D > 0$, P first increases with $\overline{G}$, reaches a maximum, and thereafter decreases, approaching an asymptotic value $P_\infty = 1/F_\infty$. There is, therefore, an optimum value of the mean gain $\overline{G}$ at which the performance factor P is maximized. This optimum value $\overline{G}_{\text{opt}}$ decreases as D increases and increases as $\sigma^2/\phi T$ increases.

The above conclusion, regarding the dependence of P on D, is based on the assumption of a fixed mean gain $\overline{G}$. Since $\overline{G}$ itself decreases with increasing D, it is perhaps more useful to examine the effect of D on P for a device with fixed multiplication-region length l. Fig. 6 is a plot of P as a function of D for a fixed value of $\sigma^2/\phi T$ and different values of the scaled length $L = \alpha l$. It is clear that for given values of L and $\sigma^2/\phi T$ there is an optimum dead space D_{opt} which maximizes P.

The role that F plays in the SNR is most important when the circuit-noise parameter $\sigma^2/\phi T$ is small in comparison with $\overline{G}$ since the decrease in F due to dead space has a beneficial effect on the SNR. On the other hand, when the ratio $\sigma^2/\phi T \overline{G}^2$ is large compared to F, then the SNR is mainly dependent on $\overline{G}$ and therefore deteriorates with increasing D.

F. Comparison Between a Dead-Space-Modified Conventional Device (DAPD) and a Multilayer (Superlattice) Device (SAPD)

Dead space tends to localize the ionizations to positions separated by at least the dead space. It is therefore of interest to compare the behavior of the dead-space-limited conventional avalanche photodiode (DAPD) with the multilayer (superlattice) avalanche photodiode (SAPD) in which ionizations occur at specific positions determined by the structure [24].

Consider an N-stage SCM SAPD for which multiplication with probability P can occur only at positions separated by distances δ. The mean gain $\overline{G}_{s1}$ and the excess noise factor F_{s1} are then given by [9]

$$\overline{G}_{s1} = (1 + P)^N \tag{28}$$

and

$$F_{s1} = 1 + \left(\frac{1 - P}{1 + P}\right) \frac{\overline{G}_{s1} - 1}{\overline{G}_{s1}}. \tag{29}$$

To compare this device with a DAPD, we assume that the two devices have the same length l and that $P = \alpha\delta$, i.e., the distributed multiplication in the conventional DAPD is equal to the lumped probability of ionization in the discrete device (SAPD). We further assume that the two devices have equal mean gain ($\overline{G}_{s1} = \overline{G}$) and compare their excess noise factors F_{s1} and F, as functions of $\overline{G} = \overline{G}_{s1}$.

By equating $\overline{G}$, which is a function of $L = \alpha l$ and $D = \alpha d$, to $\overline{G}_{s1}$, we obtain the value of δ necessary for the equivalence between the two devices. Since $\overline{G}_{s1}$ varies between $e^{\alpha l}$ and $2^{\alpha l}$ as δ varies from 0 to $1/\alpha$, and since $\overline{G}$ is upper-bounded by $e^{\alpha l}$ for any D, the comparison is considered only for gains $\overline{G}$ satisfying the inequality

$$\overline{G} \geq 2^{\alpha l}. \tag{30}$$

The results are shown in Fig. 7 for $D = 0.1$. For all values of the mean gain $\overline{G}$, F_{s1} is smaller than F. In particular, the asymptotic value of F_{s1} is given by

$$F_{s1_\infty} = 1 + \frac{1 - \Delta_\infty}{1 + \Delta_\infty} \tag{31}$$

where Δ_∞ is the solution, in the unit interval, of the equation

$$\frac{1}{\Delta_\infty} \ln(1 + \Delta_\infty) = B \tag{32}$$

and B is the scaled Malthusian parameter of the age-dependent branching process. This gives $F_{s1_\infty} = 1.42$ as compared to 1.71 for the DAPD with $D = 0.1$.

Instead of comparing the DAPD and SAPD with $\alpha\delta$ equated to P as above, we now equate the separation δ between the stages of the SAPD to the dead space d of the DAPD. As before, the two devices are taken to have the same length and the same mean gain. Equating $\overline{G}$ with $\overline{G}_{s2} = (1 + P)^{l/d}$ gives the desired value of P

$$P = (\overline{G})^{d/l} - 1. \tag{33}$$

Since in this case $\overline{G}_{s2}$ varies between 1 and $2^{l/d}$ as P varies from 0 to 1, the comparison will be considered only for gains satisfying the inequality

$$\overline{G} \leq 2^{l/d}. \tag{34}$$

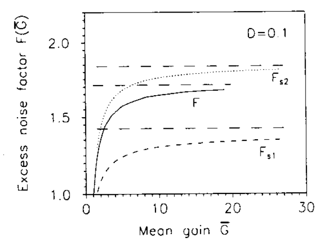

Fig. 7. Dependence of the excess noise factor F on the mean gain $\overline{G}$ for i) a DAPD with scaled dead space parameter $D = \alpha d = 0.1$ and scaled multiplication region length $L_{\overline{G}} = \alpha l_{\overline{G}}$ corresponding to a mean gain $\overline{G}$ (solid curve); ii) an SAPD with ionization probability per stage $P = \alpha\delta$ and $l_{\overline{G}}/\delta$ stages, where δ is chosen so that the mean gain $\overline{G}_{s1}$ equals the mean gain of the DAPD $\overline{G}$ (dashed curve); iii) an SAPD with $l_{\overline{G}}/d$ stages and ionization probability per stage P chosen so that the mean gain $\overline{G}_{s2} = \overline{G}$ (dotted curve).

The results are displayed in Fig. 7 for $D = 0.1$. For all values of $\overline{G}$,

$$F_{s2} = 1 + \left(\frac{1 - P}{1 + P}\right)\left(\frac{\overline{G}_{s2} - 1}{\overline{G}_{s2}}\right)$$

is greater than F. The asymptotic value of F_{s2} is given by

$$F_{s2_\infty} = 1 + \frac{1 - P_\infty}{1 + P_\infty} \tag{35}$$

where

$$P_\infty = e^{BD} - 1. \tag{36}$$

This gives $F_{s2_\infty} = 1.84$ as compared to 1.71 for the DAPD with $D = 0.1$.

In summary, the SAPD may or may not outperform the DAPD, depending on the selection of the device parameters used for the comparison.

IV. Impulse Response Function

The time course of the total current generated in the external circuit due to all the electron–hole pairs initiated by one electron at $t = 0$ is related to the stochastic process $Z(x)$ by (1d). Using the scaled variables $X = \alpha x$ and $L = \alpha l$, (1d) gives

$$i(t) = \int_0^L i_p(t, X)\, d(Z(X)) \tag{37}$$

where

$$i_p(t, X) = \frac{q}{L}\left\{ V_e \left[u\left(t - \frac{X}{V_e}\right) - u\left(t - \frac{L}{V_e}\right)\right] + V_h \left[u\left(t - \frac{X}{V_e}\right) - u\left(t - \frac{X}{V'}\right)\right]\right\}$$

$$V_e = \alpha v_e$$

and

$$\frac{1}{V'} = \frac{1}{\alpha v'} = \frac{1}{\alpha}\left(\frac{1}{v_e} + \frac{1}{v_h}\right).$$

We now examine the statistics of $i(t)$ assuming that the velocities of the carriers are everywhere the same.

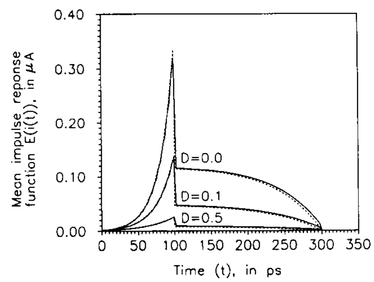

Fig. 8. Mean impulse response function $E\{i(t)\}$ for a DAPD as a function of time t, assuming $\alpha = 5000$ cm^{-1}, $l = 10$ μm, $v_e = 10^7$ cm/s, $v_h = 5 \times 10^6$ cm/s, and different values of the scaled dead space parameter $D = \alpha d$. The dotted curves represent the corresponding approximate solutions $E\{i(t)\}$, valid for $L \gg D$.

A. Mean

The mean of the impulse response function is given by

$$E\{i(t)\} = \int_0^L i_p(t, X)\, d(E\{Z(X)\}) = \int_0^L i_p(t, X)\, d(\mu(X)). \tag{38}$$

Using the results obtained earlier for $\mu(X)$, the integral in (38) was evaluated numerically and the graphs in Fig. 8 were generated for different values of the scaled dead space $D = \alpha d$, using device parameters $\alpha = 5000$ cm^{-1}, $l = 10$ μm, $v_e = 10^7$ cm/s, and $v_h = 5 \times 10^6$ cm/s. The results for the $D = 0$ case agree with those obtained previously [8, fig. 2, dashed curve]. We observe that as D increases, the magnitude of $E\{i(t)\}$ decreases everywhere, implying a reduced area (mean gain), which confirms our earlier results.

If $L \gg D$, the asymptotic value for $\mu(X)$ (see (16)) can be used in (38) to give the following analytic expression for the mean current:

$$E\{i(t)\} \approx \begin{cases} 0, & t < 0 \\ \dfrac{qV_e}{L}, & 0 \le t \le \tau_e \\ \dfrac{qC_1}{L}\left[(V_e + V_h)(e^{BV_e t} - e^{BD}) + \dfrac{V_e}{C_1}\right], & \tau_e < t \le \tau' \\ \dfrac{qC_1}{L}\left[(V_e + V_h)e^{BV_e t} - V_h e^{BV' t} - V_e e^{BD} + \dfrac{V_e}{C_1}\right], & \tau' < t \le T_e \\ \dfrac{qC_1}{L}\left[V_h(e^{BL} - e^{BV' t})\right], & T_e < t \le T_f \\ 0, & t > T_f \end{cases} \tag{39}$$

where $\tau_e = D/V_e$, $\tau' = D/V'$, $T_e = L/V_e$, and $T_f = L/V'$. The dotted curves in Fig. 8 represent the approximate behavior of $E\{i(t)\}$ given by (39) for different values of D, with $\alpha = 5000$ cm^{-1}, $l = 10$ μm, $v_e = 10^7$ cm/s, and $v_h = 5 \times 10^6$ cm/s. The agreement with the solid curves representing the exact solution is gratifying.

B. Standard Deviation

The second moment of $i(t)$ is

$$E\{i^2(t)\} = \int_0^L \int_0^L i(t, X_1) i(t, X_2) \cdot E\{d(Z(X_1))\, d(Z(X_2))\} = \int_0^L \int_0^L i(t, X_1) i(t, X_2) \frac{\partial^2}{\partial X_1 \partial X_2} \cdot R(X_1, X_2)\, dX_1\, dX_2 \tag{40}$$

where $R(X_1, X_2)$ is the autocorrelation function of the process $Z(X)$. Using the asymptotic expression for $R(X_1, X_2)$ given in (22), we obtain

$$E\{i^2(t)\} \approx \frac{C_2}{C_1^2}\left[E\{i(t)\}\right]^2 \quad (L \gg D). \tag{41}$$

With the help of (21), the variance of $i(t)$ is then

$$\mathrm{var}(i(t)) \approx (F_\infty - 1)\left[E\{i(t)\}\right]^2 \quad (L \gg D). \tag{42}$$

Thus the signal-to-noise ratio SNR, $[E\{i(t)\}]^2/\mathrm{var}(i(t))$, is a constant equal to $(F_\infty - 1)^{-1}$, that is independent of time. Fig. 9 is a plot of $E\{i(t)\}$ when $L \gg D$ for different values of D, with $\alpha = 5000$ cm^{-1}, $l = 10$ μm, $v_e = 10^7$ cm/s, and $v_h = 5 \times 10^6$ cm/s, together with its one standard deviation (SD) limits (shaded region), i.e., $E\{i(t)\} \pm \sqrt{\mathrm{var}(i(t))}$. It is seen that as D increases, the SNR increases everywhere as a result of the decrease in F_∞ as discussed earlier.

V. Conclusion

Dead space has important effects on the noise properties of continuous multiplication APD's. Using an age-dependent branching process approach, we found that dead

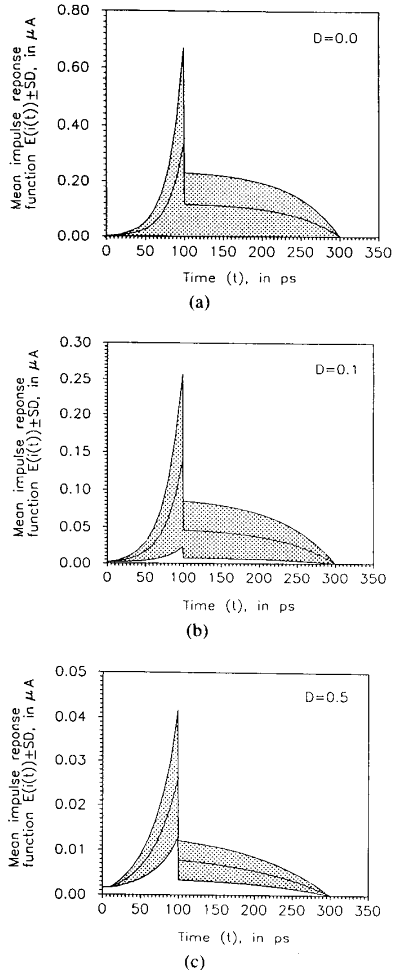

Fig. 9. Mean impulse response function $E\{i(t)\}$ for a DAPD as a function of time t, assuming $\alpha = 5000\ \text{cm}^{-1}$, $l = 10\ \mu\text{m}$, $v_e = 10^7$ cm/s, $v_h = 5 \times 10^6$ cm/s, along with its one standard deviation (SD) limits for different scaled dead space parameters $D = \alpha d$: (a) $D = 0$, (b) $D = 0.1$, (c) $D = 0.5$. The results are valid for $L \gg D$.

space reduces both the mean gain and the excess noise factor. Dead space also affects the time dynamics of the response, by reducing the mean and standard deviation of the impulse response function for all times. Inasmuch as real devices have an intrinsic dead space built into them, the results reported here may therefore elucidate some enigmatic results in the literature [27].

To evaluate the effect of dead space on the performance of APD's, we have determined the signal-to-noise ratio (SNR) of an optical receiver that includes the effect of photon noise and electronic circuit noise. The SNR was compared for two receivers using APD's of the same mean gain, one without dead space and the other with dead space. It was found that the presence of dead space improved the SNR. For a given dead space parameter $D = \alpha d$, α being the ionization coefficient and d being the dead space, there is an optimum mean gain for which the SNR is maximized, if all other parameters are fixed. We also found that an optimum value of the dead space parameter D exists at which the SNR is maximized for a device with a fixed multiplication-region length. Apparently, the reduction in the noisy clusters achieved by the dead space outweighs the attendant loss of carriers.

Two comparisons between a conventional APD with dead space (DAPD) and a superlattice APD (SAPD) were carried out based on the SNR. In the first comparison we assumed that the two devices had equal multiplication-region lengths and equal mean gains, with the SAPD having an ionization probability of $P = \alpha\delta$ per stage, where δ is the length of each stage. In this case, the performance of the SAPD was found to be superior to the DAPD. In the second comparison we assumed again that the two devices had equal multiplication-region lengths and equal mean gains, but the stages of the SAPD were separated by the distance d, the dead space of the DAPD. In this case, the performance of the DAPD was superior to that of the SAPD.

We conclude that the SAPD may or may not outperform the DAPD depending on the selection of the device parameters used for the comparison.

Acknowledgment

The authors wish to thank R. J. McIntyre for valuable discussions.

References

[1] R. J. McIntyre, "Multiplication noise in uniform avalanche diodes," *IEEE Trans. Electron Devices*, vol. ED-13, pp. 164–168, 1966.

[2] ——, "The distribution of gains in uniformly multiplying avalanche photodiodes: Theory," *IEEE Trans. Electron Devices*, vol. ED-19, pp. 703–713, 1972.

[3] J. Conradi, "The distribution of gains in uniformly multiplying avalanche photodiodes: Experimental," *IEEE Trans. Electron Devices*, vol. ED-19, pp. 713–718, 1972.

[4] P. P. Webb, R. J. McIntyre, and J. Conradi, "Properties of avalanche photodiodes," *RCA Rev.*, vol. 35, pp. 234–278, 1974.

[5] S. D. Personick, "New results on avalanche multiplication statistics with applications to optical detection," *Bell Syst. Tech. J.*, vol. 50, pp. 167–189, 1971.

[6] ——, "Statistics of a general class of avalanche detectors with application to optical communication," *Bell Syst. Tech J.*, vol. 50, pp. 3075–3095, 1971.

[7] M. C. Teich, K. Matsuo, and B. E. A. Saleh, "Time and frequency response of the conventional avalanche photodiode," *IEEE Trans. Electron Devices*, vol. ED-33, pp. 1511–1517, 1986.

[8] K. Matsuo, M. C. Teich, and B. E. A. Saleh, "Noise properties and time response of the staircase avalanche photodiode," *IEEE Trans. Electron Devices*, vol. ED-32, pp. 2615–2623, 1985.

[9] M. C. Teich, K. Matsuo, and B. E. A. Saleh, "Excess noise factors for conventional and superlattice avalanche photodiodes and photomultiplier tubes," *IEEE J. Quantum Electron.*, vol. QE-22, pp. 1184–1193, 1986.

[10] K. F. Brennan, Y. Wang, M. C. Teich, B. E. A. Saleh, and T. Khorsandi, "Theory of the temporal response of a simple multiquantum-well avalanche photodiode," *IEEE Trans. Electron Devices*, vol. 35, pp. 1456–1467, 1988.

[11] N. Z. Hakim, B. E. A. Saleh, and M. C. Teich, "Generalized excess noise factor for avalanche photodiodes of arbitrary structures," *IEEE Trans. Electron Devices*, vol. 37, pp. 599–610, Mar. 1990.

[12] Y. Okuto and C. R. Crowell, "Ionization coefficients in semiconductors: A nonlocalized property," *Phys. Rev., B.*, vol. 10, pp. 4284–4296, 1973.

[13] ——, "Threshold energy effect on avalanche breakdown voltage in semiconductor junctions," *Solid State Electron.*, vol. 18, pp. 161–168, 1975.

[14] R. A. LaViolette, "Oscillatory transients in a non-Markovian random walk," *J. Chem. Phys.*, vol. 89, pp. 6905-6911, 1988.
[15] R. A. LaViolette and M. G. Stapelbroek, "A non-Markovian model of avalanche gain statistics for a solid-state photomultiplier," *J. Appl. Phys.*, vol. 65, pp. 830-836, 1989.
[16] K. B. Athreya and P. E. Ney, *Branching Processes.* Berlin, FRG: Springer, 1972.
[17] T. E. Harris, *The Theory of Branching Processes.* Berlin, FRG: Springer, 1963.
[18] S. Karlin and H. Taylor, *A First Course in Stochastic Processes.* New York, NY: Academic Press, 1975.
[19] R. Chin, N. Holonyak, G. E. Stillman, J. Y. Tang, and K. Hess, "Impact ionization in multilayered heterojunction structures," *Electron. Lett.*, vol. 16, pp. 467-469, 1980.
[20] G. F. Williams, F. Capasso, and W. T. Tsang, "The graded bandgap multilayer avalanche photodiode: A new low-noise detector," *IEEE Electron Device Lett.*, vol. EDL-3, pp. 71-73, 1982.
[21] F. Capasso, W. T. Tsang, A. L. Hutchinson, and G. F. Williams, "Enhancement of electron impact ionization in a superlattice: A new avalanche photodiode with a large ionization rate ratio," *Appl. Phys. Lett.*, vol. 40, pp. 38-40, 1982.
[22] H. Blauvelt, S. Margalit, and A. Yariv, "Single-carrier-type dominated impact ionization in multilayer structures," *Elect. Lett.*, vol. 18, pp. 375-376, 1982.
[23] F-Y Juang, U. Das, Y. Nashimoto, and P. K. Bhattacharya, "Electron and hole impact ionization coefficients in GaAs-$Al_xGa_{1-x}As$ superlattices," *Appl. Phys. Lett.*, vol. 47, pp. 972-974, 1985.
[24] F. Capasso, "Physics of avalanche photodiodes," in *Semiconductors and Semimetals*, R. K. Willardson and A. C. Beer, Series Eds., vol. 22, pt. D, *Lightwave Communications Technology*, W. T. Tsang, Ed. New York, NY: Academic Press, 1985, pp. 1-172.
[25] M. Zirngibl, J. C. Bischoff, D. Theron, and M. Ilegems, "A superlattice GaAs/InGaAs-on-GaAs photodetector for 1.3-μm applications," *IEEE Electron Device Lett.*, vol. 10, pp. 336-338, 1989.
[26] S. D. Personick, *Fiber Optics.* New York, NY: Plenum, 1985.
[27] S. Miura, T. Mikawa, H. Kuwatsuka, N. Yasuoka, T. Tanahashi, and O. Wada, "AlGaSb avalanche photodiode exhibiting a very low excess noise factor," *Appl. Phys. Lett.*, vol. 54, pp. 2422-2423, 1989.

*

Bahaa E. A. Saleh (M'73-SM'86) received the B.S. degree from Cairo University, Cairo, Egypt, in 1966 and the Ph.D. degree from the Johns Hopkins University, Baltimore, MD, in 1971, both in electrical engineering.

From 1971 to 1974, he was an Assistant Professor at the University of Santa Catarina, Brazil. Thereafter, he joined the Max Planck Institute in Goettingen, Germany, where he was involved in the research of laser light scattering and photon correlation spectroscopy. He is presently Professor and Chairman of the Electrical and Computer Engineering Department at the University of Wisconsin, Madison, where he has been since 1977. He held visiting appointments at the University of California, Berkeley, in 1977, and the Columbia Radiation Laboratory of Columbia University, New York, NY in 1983. He is currently involved in the research of image processing, optical information processing, statistical optics, optical communication, and vision. He is the author of *Photoelectron Statistics* (Springer, 1978) and a co-editor of *Transformations in Optical Signal Processing* (SPIE, 1981). During 1980-1983, he was an associate editor of the *Journal of the Optical Society of America*, and during 1983-1988, he was a topical editor of the same journal. He is a member of the Board of Editors of *Quantum Optics*.

Dr. Saleh is a Fellow of the Optical Society of America and a member of Phi Beta Kappa and Sigma Xi. He received the Wisconsin Romnes Award in 1981 and was appointed a Guggenheim Fellow in 1984.

*

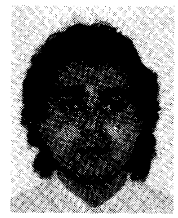

Majeed M. Hayat (S'89) was born in Kuwait on April 24, 1963. He received the B.S. degree, *summa cum laude*, from the University of the Pacific, Stockton, CA, in 1985 and the M.S. degree in 1988 from the University of Wisconsin, Madison, both in electrical engineering. He is currently working toward the Ph.D. degree at the University of Wisconsin.

His research interests include studying the performance of optical communication systems that use avalanche photodiodes as well as investigating the effect of energy buildup time on the statistical properties of avalanche photodiodes.

*

Malvin C. Teich (S'62-M'66-SM'72-F'89) was born in New York City. He received the S.B. degree in physics from the Massachusetts Institute of Technology, Cambridge, in 1961, the M.S. degree in electrical engineering from Stanford University, Stanford, CA, in 1962, and the Ph.D. degree in quantum electronics from Cornell University, Ithaca, NY, in 1966.

In 1966, he joined the MIT Lincoln Laboratory, Lexington, MA, where he was engaged in work on coherent infrared detection. In 1967, he became a member of the faculty in the Department of Electrical Engineering, Columbia University, New York, NY where he is now teaching and pursuing his research interests in the areas of quantum optics, optical and infrared detection, and sensory perception. He served as Chairman of the Department from 1978 to 1980. He is also a member of the faculty in the Department of Applied Physics and a member of the Columbia Radiation Laboratory, the Center for Telecommunications Research, and the Fowler Memorial Laboratory at the Columbia College of Physicians and Surgeons. He has authored or coauthored some 150 technical publications and holds one patent.

Dr. Teich was the recipient of the IEEE Browder J. Thompson Memorial Prize Award for his paper "Infrared Heterodyne Detection," in 1969 and in 1981, he received a Citation Classic Award of the Institute for Scientific Information for this work. He received a Guggenheim Fellowship in 1973. He is a Fellow of the American Physical Society, the Optical Society of America, and the American Association for the Advancement of Science. He is a member of Sigma Xi, Tau Beta Pi, the Acoustical Society of America, and the Association for Research in Otolaryngology. He served as a member of the Editorial Advisory Panel for the journal *Optics Letters* from 1977 to 1979 and is currently Deputy Editor of the journal *Quantum Optics* and a member of the Editorial Board of the *Journal of Visual Communication and Image Technology*.